Two-Layer Model for the

Heat Transfer to Supercritical CO$_2$

E. Laurien, S. Pandey, and D. M. McEligot*

University of Stuttgart / Institute of Nuclear Technology and Energy Systems
Pfaffenwaldring 31, D-70569 Stuttgart, Germany.
+49 711 685 62415, Laurien@ike.uni-stuttgart.de
* Nuclear Engineering Division, Univ. Idaho, 995 University Blvd., Idaho Falls, Idaho 83401
USA

Topic: sCO$_2$ Fluid Mechanics & Heat Transfer

Abstract: Heat transfer to CO$_2$ at super-critical pressure (sCO$_2$) within small-diameter (2-5 mm) pipes or channels of a compact heat exchanger must be predicted accurately in order to ensure its reliability under various operation conditions. Complex nonlinear behaviour of the heat transfer is observed due to the large variations of the sCO$_2$ properties with the local fluid temperature. Deterioration of the heat transfer may occur under conditions when a layer of low-conductivity laminar fluid near the channel walls increases in thickness due to flow acceleration and/or buoyancy. The classical two-layer model, taking account of the 'turbulent core layer' and a 'laminar sub-layer', is extended to capture these effects. New parameters of the extended model, in particular a modified thickness of the laminar sub-layer, are calibrated using results of Direct Numerical Simulations of heated sCO$_2$-pipe flows. Our new model is applied to small channels under heating or cooling conditions at 8 and 20 MPa in the temperature range between 32°C and 165°C, as relevant for a sCO$_2$ power cycle. It is shown that predictions for the heat transfer and the wall shear stress in vertical channels of the low-temperature recuperator and the reject-heat exchanger deviate significantly from standard correlations.

1. Introduction

The modified recuperative Brayton cycle with sCO$_2$ establishes an attractive thermal energy-generation process with high net efficiency of 47 % at a maximum temperature of only 650°C [1]. The cycle has a high-pressure section at 200 bars (20 MPa) and a low-pressure section at 77 bars (7.7 MPa). It requires the design of compact heat exchangers with cooled channels on the low-pressure side having bulk temperatures between 165°C and 32°C and with heated channels on the high-pressure side having temperatures between 61.1°C and 157.1°C. These compact heat exchangers consist of a metal block with small channels or pipes (hydraulic diameter about 2

mm) in which a turbulent flow of sCO_2 exists. Some of them operate near the critical point of CO_2 (32.9°C and 7.48 MPa). The flow in theses channels can be vertically upward, downward or horizontal. Heat transfer and friction should be predicted accurately for the design method.

Typically, experiments with sCO_2 in small vertical pipes have been performed with a constant wall-heat flux induced by electrical heating of the pipe walls [2, 3]. As a consequence of the strong property variation of sCO_2 with temperature such flows may, under the influence of buoyancy and acceleration, exhibit complex and sometimes unexpected local behaviour such as heat transfer 'enhancement' or 'deterioration' [4]. Similar phenomena may also exist in turbulent cooled pipe flow, but only few experiments under cooling conditions are available. To predict the local wall temperature empirical correlations of experimental data are available [5]. However, uncertainties of these methods exist. Measurements of the local wall shear stress as functions of the longitudinal coordinate are not feasible. Criteria for deterioration are discussed in [6].

An important parameter to characterize fluid turbulence locally at an axial position in the pipe is the local bulk-Reynolds number $\mathrm{Re}_b = \rho_b \, u_m D / \mu_b$, where ρ_b and μ_b are the local fluid density and the viscosity in the turbulent core, and u_m is the mean velocity. The Reynolds number is in the order of 6000 to 3×10^4. A way to investigate turbulent flows in this Reynolds-number range is by Direct Numerical Simulation (DNS), see [7, 8]. DNS is based on an accurate numerical integration of the unsteady conservation equations of mass, momentum and energy on a very fine numerical grid. Since all scales of turbulence are numerically resolved, a turbulence model is not necessary. However, DNS requires extensive computer resources and can today only be performed to study a small number of characteristic cases.

A practical way to model flow and heat transfer of circular pipe flows is the classical two-layer model, see e.g. [9]. Here, the assumption is made that the shear stress and the heat flux are constant in the direction perpendicular to the pipe walls. The flow and heat transfer in the so called turbulent 'core layer' and the laminar 'sub-layer' can be modelled analytically for constant fluid properties. In combination with a mixing-length turbulence model, this method has provided valuable insight into the heat transfer of constant-property flows [10]. Results of this theory are used today for a wide range of different fluids [11]. Accurate results are obtained only when a distinction is made between the thicknesses of the laminar 'viscous sub-layer' for the velocity and the laminar 'conducting sub-layer' for the temperature [10, 11].

The two-layer model is also attractive for variable-property flows. The idea to extend it to super-critical water has first been presented in [12] for water flows with rough walls. The capability of the method to capture heat transfer deterioration has been demonstrated for supercritical water [12]. In the present paper the two-layer model is applied to sCO_2 flows with some modifications, which are introduced to improve its accuracy. The coupling of the momentum and energy equations in the two-layer model requires information both about the wall shear stress and the wall temperature, simultaneously. A detailed determination of important parameters such as the thickness of the viscous and the conducting sub-layers had so far failed, but new

DNS data have now become available [8], which can serve as bases for model improvement.

In the present work we use the new DNS data [8] for the determination of parameters in a modified version of the two-layer model. Our new method is applied to various cases of flow conditions relevant for the 'advanced design' of the supercritical carbon-dioxide power cycle [1] in order to investigate the characteristics of these flows. A comparison of the two-layer model to sCO₂ experiments [3] is also presented.

2. Two-Layer Model for Circular Pipe Flows of sCO₂

2.1 Model Equations

At each axial position, corresponding to its average or 'bulk' enthalpy h_b, the two-layer model integrates the momentum and energy equations locally in direction y perpendicular to the wall under simplifying assumptions. The flow conditions for each calculation are defined by five additional parameters: the pressure p, the mass flux per unit area G, the wall heat flux per unit area q_w, the pipe diameter $D = 2R$, and the inlet temperature T_{in}. For small relative roughness, the wall of narrow channels can be regarded as hydraulically smooth. The flow is subdivided into a turbulent 'core layer' ('logarithmic-layer') and a laminar 'sub-layer' adjacent to the wall. In [10, 11] a laminar sub-layer for the velocity, denoted as the 'viscous sub-layer', and a laminar sub-layer for the temperature, denoted as the 'conducting sub-layer', each with its own thickness, are defined. Non-dimensional quantities are used and referred to as 'wall units'. For their definitions in the context of the core layer we use the bulk properties [12], i.e. the fluid properties at bulk temperature. For their definition in the context of the viscous/conducting sub-layers we use the wall properties [12], i.e. the fluid properties at wall temperature. The wall temperature and the wall-shear stress necessary to define these units, are a priori unknown. Therefore, iteration must be employed.

Our Excel procedure, here explained for a heated case, begins with the initialization of the iteration procedure for each bulk enthalpy h_b. First, the bulk temperature T_b, the bulk dynamic viscosity μ_b, the bulk density ρ_b, the bulk heat conductivity k_b, the bulk heat capacity for constant pressure c_{pb}, the bulk thermal expansion coefficient β_b, the mean velocity u_m, the local bulk-Reynolds number $\mathrm{Re}_b = \rho_b u_m D / \mu_b$, and the bulk Prandtl number $\mathrm{Pr}_b = \mu_b c_{pb} / k_b$ are determined using the program REFPROP [13]. Estimates for wall shear stress $\tau_w = \rho_b u_m^2 \lambda / 8$ from the empirical Blasius equation [10] for the pipe friction coefficient $\lambda = 0.31 / \sqrt[4]{\mathrm{Re}_b}$ and for wall temperature $T_w = T_b + q_w D / (Nu \times k_b)$ from the empirical Dittus-Boelter correlation [10] for the Nusselt number $Nu = 0.023 \mathrm{Re}_b^{0.8} \mathrm{Pr}_b^{0.4}$ are provided.

The next step is the determination of the changes of the velocity and the temperature across the turbulent core layer. Since the bulk properties are used, therefore both quantities are independent of the wall temperature. The velocity at the edge of the viscous sub-layer and the temperature at the edge of the conducting sub-layer are computed. Let us define the wall units for the turbulent core layer as

$$u^{+b} = \frac{\bar{u}}{u_{\tau b}} \quad ; \quad y^{+b} = \frac{y\,\rho_b\,u_{\tau b}}{\mu_b} \quad ; \quad u_{\tau b} = \sqrt{\frac{\tau_w}{\rho_b}} = \sqrt{\frac{\lambda}{8}}\,u_m \quad (1)$$

According to the constant-property logarithmic law of the wall, the velocity difference across the turbulent core layer is

$$\Delta u_{turb}^{+b} = \frac{1}{\kappa}\left(\ln R^{+b} - \ln y_{vs}^{+b}\right) \quad (2)$$

with the von-Karman constant $\kappa = 0.41$ and the thickness of the viscous sub-layer $y_{vs}^{+b} = 11.8$ [10].

For a power-law velocity profile $u^{+b} = 8.6 \cdot (y^{+b})^{1/7}$, which is a good approximation of the logarithmic law of the wall at high Reynolds numbers [10], the relation between the mean and the centre-line velocity u_{cl}^{+b} is

$$u_m^{+b} = \frac{8.6}{\pi R^{+b2}} \int_{R^{+b}}^{0} \left(R^{+b} - r^{+b}\right)^{1/7} 2\pi\,r^{+b}d(-y^{+b}) = 0.8167\,u_{cl}^{+b} \quad (3)$$

The mean velocity can be calculated by assuming contact mass flux. The velocity at the edge of the viscous sub-layer can then be determined from the velocity u_{cl} at the centre-line of the pipe by

$$u_{vs} = u_{cl} - \Delta u_{turb} \quad (4)$$

Next, the temperature T_{cs} at the edge of the conducting sub-layer is determined. The non-dimensional temperature in wall units is defined as

$$T^{+b} = \frac{(T - T_w)u_{\tau b}}{q_w / \rho_b\,c_{pb}} \quad (5)$$

According to the two-layer model, the temperature difference across the turbulent core layer is

$$\Delta T_{turb}^{+b} = \frac{\mathrm{Pr}_T}{\kappa}\left(\ln R^{+b} - \ln y_{cs}^{+b}\right) \quad , \quad (6)$$

where y_{cs}^{+b} is the non-dimensional thickness of the conducting sub-layer and $\mathrm{Pr}_T = 0.85$ is the turbulence Prandtl number.

With the assumption $T_{cl} \approx T_b$, we get the temperature at the edge of the conducting sub-layer

$$T_{cs} = T_b + \Delta T_{turb} \tag{7}$$

The non-dimensional sub-layer thickness y_{cs}^{+b} is modelled consistent with the constant-property theory [7, 8] as

$$y_{cs}^{+b} = \frac{y_{vs}^{+b}}{\mathrm{Pr}_w^{1/3}} \tag{8}$$

The wall-Prandtl number Pr_w is determined from the estimation of the wall temperature above. Eqs. (1) – (8) establish the initialization part of our method.

In the following the iteration part of our method is described. For improved accuracy the viscosity at the wall is replaced by its average across the viscous sub-layer. The wall shear stress follows from the laminar friction law within the viscous sub-layer

$$\tau_w = \mu \left. \frac{du}{\partial y} \right|_w \approx \left(\mu_w + \mu_{vs} \right) \frac{u_{vs}}{2 y_{vs}} \tag{9}$$

The non-dimensional thicknesses of the viscous sub-layer y_{vs}^{+w} and of the conduction sub-layer y_{cs}^{+w} are based on wall-properties, i.e., the index 'b' in eq. (1) is replaced by the index 'w'.

The temperature difference across the conducting sub-layer is most accurately estimated by using the 'thermal-resistance' analogy [14]. A new state variable is defined

$$\omega(T) = \int_{T_{ref}}^{T} k(T) \, dT \tag{10}$$

The relation between ω and T is provided by a 'lookup table' with an arbitrary reference temperature T_{ref}. In this work we use T_{ref} = -20 °C. The wall temperature follows indirectly from

$$q_w y_{cs} = \omega(T_w) - \omega(T_{cs}) \tag{11}$$

The quantities y_{vs}^{+w} and y_{cs}^{+w} are modified below in sect 2.3 in order to take account of important physical effects due to property variation such as acceleration and buoyancy.

Eqs. (8) – (10) must be repeated until converged, i.e., the wall temperature and the wall shear stress remain constant during final iterations. We use a constant number of nine iterations, which appeared to be sufficient at a first glance. To avoid a possible instability of the iteration, under-relaxation with a factor of 0.5 is used, but no detailed investigation or optimization of this iteration procedure was performed. In some computations the wall shear stress became negative, in particular under cooling conditions near the critical pressure, e.g. at 7.7 MPa. These results are not presented in this paper, because the limitations of the theory are exceeded.

2.2 Comparison to Experimental Data

The above discussed theory is used in [15] to model the experiments of Kim et al. [3] at 7.75 MPa, see Figure 1. The model is able to predict the measured sharp rise of the wall temperature only qualitatively. This 'deterioration' occurs, when the wall temperature reaches the 'pseudo-critical' value of T_{pc} = 33.2°C, where the changes of the sCO$_2$-properties with temperature and the heat capacity are at their maximum.
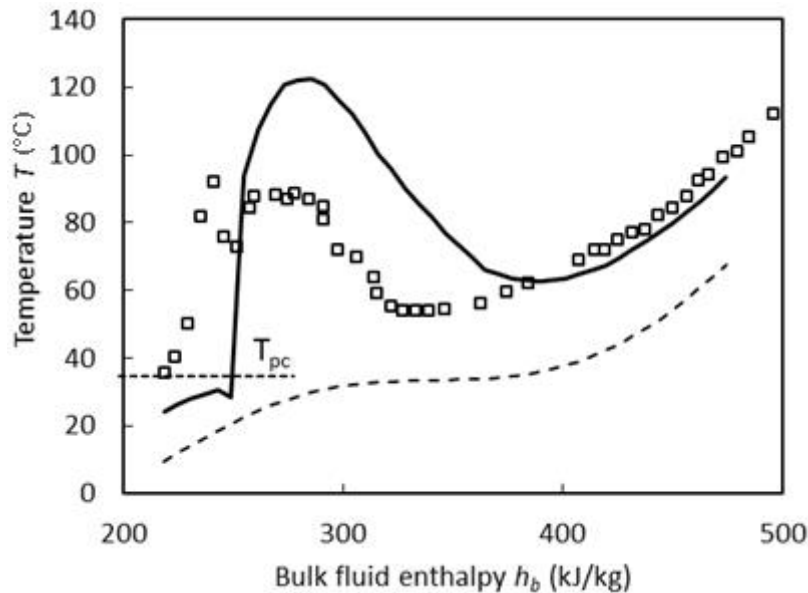

Figure 1: Comparison of the wall temperature (full line) obtained with the two-layer model to experiments [3] (symbols) [3], D = 4.4 mm, G = 400 kg/m^2 and q$_w$ = 50 kW/m^2. The dashed lines indicates the bulk temperature and the pseudocritical temperature T_{pc}

However, the maximum temperature of 120°C predicted by the model is higher than the measured maximum temperature of 95°C and there is a shift of 20 *kJ/kg* in the predicted onset of deterioration towards a larger enthalpy. The reason for this may be the inability of the model, described so far, to capture important physical effects such as acceleration and buoyancy. For example, acceleration may lead to re-laminarization of the flow and associated to an increase of the thickness of the conducting sub-layer. Furthermore, it became obvious [15], that for lower wall-heat flux the onset of deterioration cannot be predicted accurately. Therefore, the accuracy and reliability of the model must be improved. Since the present case is not relevant for the sCO$_2$ power cycle due to its large pipe diameter, it is not presented further.

2.3 Model Improvement

In order to improve our model generally, the Direct Numerical Simulation (DNS) results of [8] serve as a data base. Compared to experiments DNS results have the advantage that the local wall shear stress is available in addition to the wall temperature.
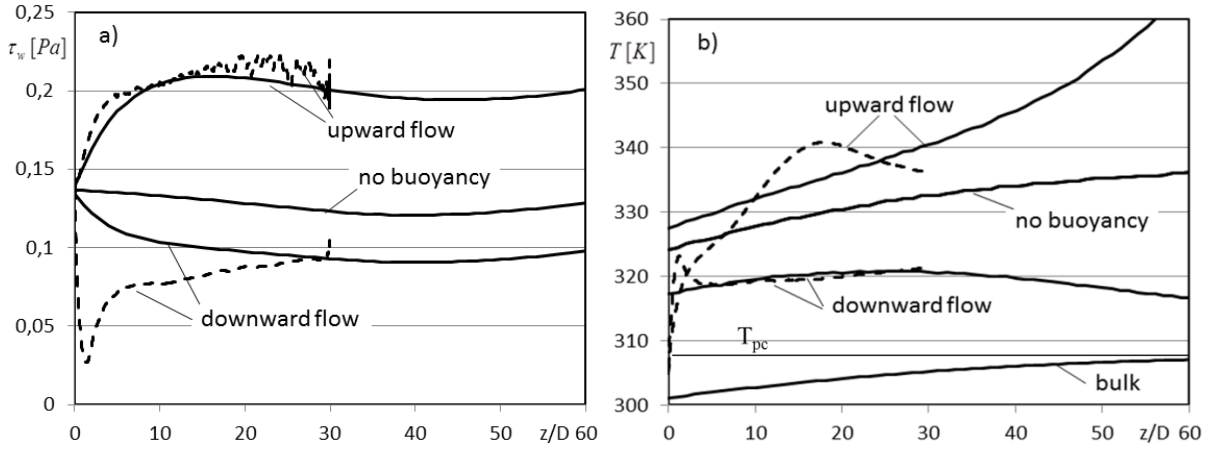
Figure 2: Comparison of our predictions using the two-layer model (full lines) with results of the DNS [8] (dashed lines) at $p = 8\,MPa$, $D = 2mm$, $G = 166\,kg/m^2 s$, $q_w = 10.8\,kW/m^2$ and $T_{in} = 28°C$. The flow is with buoyancy upward, downwad or with no buoyancy.

The non-dimensional thicknesses of the laminar sub-layer y_{vs}^{+w} and the conducting sub-layer y_{cs}^{+w} are modified from their original values of sect 2.1. Each modification aims to model a particular physical effect, which is observed in the DNS: (i) re-laminarization (due to flow acceleration), (ii) the 'internal' (structural) and (iii) the 'external' (on the mean velocity profile) effect of buoyancy.

Figure 2 shows the wall shear stress and the wall temperature for two cases, which were simulated with DNS [8]. An additional case considers acceleration, but 'no buoyancy', i.e., the gravity acceleration *g* is artificially set to zero in the simulation. This is done for reference in order to separate the acceleration effects from the buoyancy effects. The following modifications of the model of sect 2.1 were applied:

To model (i) re-laminarization due to flow acceleration the thickness of the viscous sub-layer is increased proportional to the non-dimensional acceleration parameter K_v [6] to fit DNS data empirically, based on bulk properties:

$$y_{vs}^{+w} = 11.8 + c_v K_v \quad ; \quad K_v = \frac{4q_w \mu_b u_m}{GD\rho_b^2} \left.\frac{\partial \rho}{\partial h}\right|_b \quad ; \quad \left.\frac{\partial \rho}{\partial h}\right|_b = \frac{\rho_b \beta_b}{c_{pb}} \tag{12}$$

with $c_v = 1.4 \times 10^7$ for both upward and downward flow. This leads to a decrease of the wall shear stress compared to a non-accelerated case (not shown). The result is presented in Figure 2 marked with 'no buoyancy'. The conducting sub-layer is not modified. The wall temperature remains the same as in the original model.

Next (ii), the internal (structural) effect of buoyancy is modelled by a modification of the thickness of the conducting sub-layer

$$y_{cs}^{+w} = \frac{11.8}{Pr_{cs}^{1/3}} - c_{buoy,in} \cdot Ri_b \quad ; \quad Ri_b = \frac{Gr_b}{Re_b^2} \tag{13}$$

7

with $c_{buoy,in} = 140$ for downward $c_{buoy,in} = -30$ for upward flow. This leads to an increase (upward flow) or a decrease (downward flow) of the wall temperature. The sign of the parameter $c_{buoy,in}$ is explained as follows: for downward flow the flow is thermally unstable resulting in a production of thermal turbulence and therefore in a decrease of the thickness of the conducting sub-layer. For upward flow the flow is thermally stable and turbulence is damped, which is modelled by an increase of the conducting sub-layer thickness. To model these effects the bulk Richardson number is taken as the relevant model parameter. Due to the change in temperature the shear stress is also affected, but the changes were small (not shown). In the upward case the DNS data show a 'wave' (or oscillation) with a wave-length of about 10 D. The origin of this wave is not fully understood yet and therefore it is not modelled here. In the downward case a local maximum of the wall temperature near z/D = 2 is also not modelled, because it is considered an inlet effect, which is beyond the capabilities of the two-layer model for developed flows.

The external effect of buoyancy on the mean flow profile (iii) is modelled by modification of the wall-shear stress. We consider a modified wall shear stress as the consequence of a shear-induced contribution as calculated in eqs. (9) and an additional buoyancy-induced contribution

$$\tau_{w,mod} = \tau_w + \left(c_{buoy,ex} \times 10^{-7} \, Gr_w\right)\left(1 - e^{-z/5D}\right) \quad , \quad Gr_w = \frac{g\beta_w \, \rho_w^2 D^3 |T_b - T_w|}{\mu_w^2} \quad , \quad (14)$$

with $c_{buoy,ex} = 0.2 Pa$ for upward $c_{buoy,ex} = -0.05 Pa$ for downward flow. The buoyancy-induced wall shear stress may be interpreted as a result of a circulating natural convection flow superposed to the longitudinal forced convection, leading to 'M-shaped' velocity profiles in upward flow. The convection flow is modelled as a function of the wall-Grashof number. In upward-flow the DNS data are well approximated. In the downward case, however, some details are not captured accurately. Here, further improvement of our model is necessary. The term with the exponential function in eq. (14) models a short distance, which is assumed to be necessary for the convection flow to become established.

A comparison of the upward and downward flow cases in the region far downstream in Figure 2 suggests, that the upward flow leads to a further increase of the wall temperature, denoted as 'deterioration' whereas the downward-flow case does not. This is an often-observed phenomenon in flows at super-critical pressure.

The numerical values of $c_{buoy,in}$ and $c_{buoy,out}$ fit the DNS in the best possible way. We are aware, that using only two DNS cases may not be sufficient to establish an accurate model for a wide range of flow conditions. However, the computation of additional cases to provide a larger DNS-data base is underway [16].

3. Application to a sCO2-Compact Heat Exchangers

In this chapter our method is applied to cases relevant for the supercritical CO_2 power cycle [1]. We consider vertical upward or downward flow within channels with

a hydraulic diameter of 2 mm. The wall is either upward or downward and heated or cooled, leading to the stability behaviour summarized in Table 1.

Table 1: Thermal stability table of vertical pipe flow

	heated	cooled
upward flow	stable	unstable
downward flow	unstable	stable

The stable cases tend toward development of an M-shaped velocity profile. For these, the additional wall shear stress is positive, otherwise negative. The heated flow is accelerated and therefore re-laminarization occurs. In order to promote the understanding of the flow, we further assume constant wall heat flux, although this is not the case in a heat exchanger. Our method is not applicable for horizontal flow, because strong density stratification occurs, as the DNS [16] indicates.

3.1 Low-Temperature Recuperator at the High-Pressure Side

The flow is heated at 200 bars [1], where sCO_2 behaves practically like a gas flow. The flow may be upward or downward, depending on the design of the recuperator. The wall temperature by proposed two layer model is shown in Figure 3 (for upward flow) and Figure 4 (for downward flow)
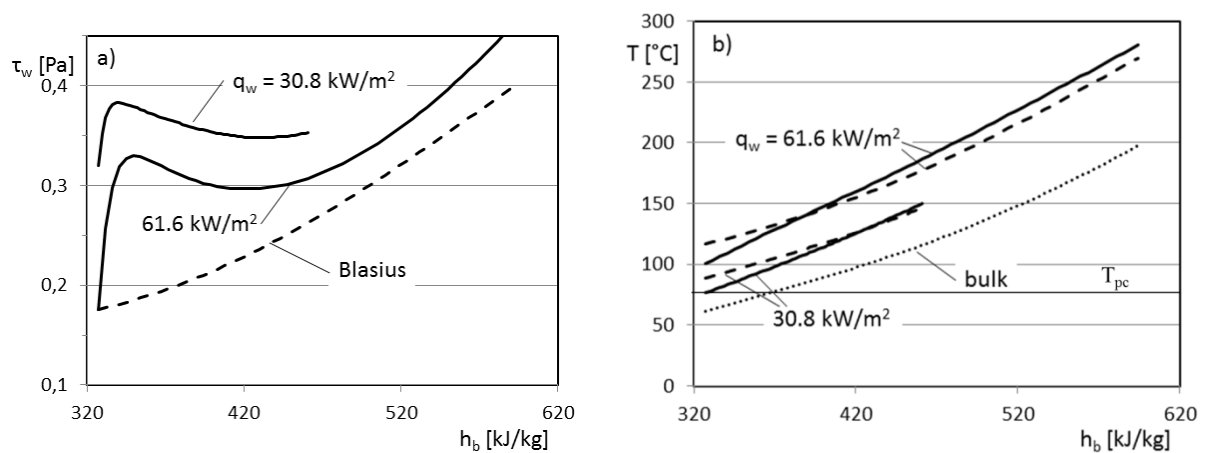

Figure 3: a) Wall shear stress and b) wall temperature for upward flow, two wall heat fluxes, p = 20 MPa, D = 2 mm, G = 166 kg/m^{2}s, T_{in} = 61.1 °C, a) wall shear stress (full line) and comparison to the Blasius correlation (dashed line), b) wall temperature (full line) and comparison with the Dittus-Boelter correlation (dashed line)

The wall temperature is almost the same as predicted by the Dittus-Boelter correlation, but the wall shear stress shows significant deviation from the constant-property prediction due to buoyancy.
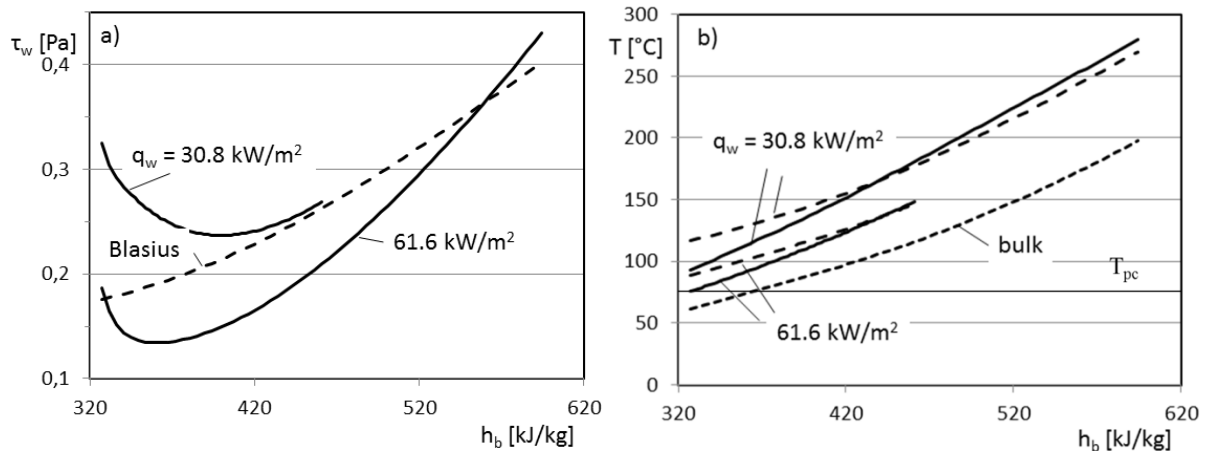
Figure 4: same as figure 3 for downward flow

3.2 Low-Temperature Recuperator at the Low-Pressure Side

The flow of the low-pressure side is cooled, i.e., in Figure 5 the flow is from right to left. Compared to the previous cases we have lowered the wall heat flux, because for higher heat flux negative values of the wall shear stress occur, for which our theory does not apply. We also changed the pressure from 77 to 80 bars for the same reason.

The wall temperature predicted by our method deviates significantly from the prediction of the Dittus-Boelter correlation. For the wall shear stress a large deviation occurs as well. These changes are due to the combined effects of buoyancy and variable properties. Re-laminarization due to acceleration does not occur, because a cooled flow is not accelerated. The wall temperature is the same for upward or downward flow. The reason for same temperature is that effects of buoyancy are not significant. We have calculated Gr_b/Re_b^2 as criterion for buoyancy, if its value is more than 10^{-2}, then buoyancy effects are significant [17]. But in both the cases its magnitude is in the range of 10^{-4}.

3.3 Reject-Heat Exchanger at the Low-Pressure Side

The flow on the sCO_2-side is cooled. We also changed the pressure from 77 to 80 bars. Figure 6 shows a sharp rise of the wall shear stress between 400 and 450 kJ/kg for downward flow. In this case, buoyance parameter Gr_b/Re_b^2 is ranging from 10^{-2} to 10^{-4}, which explains difference in temperature at the outlet between 375 and 306 kJ/kg.
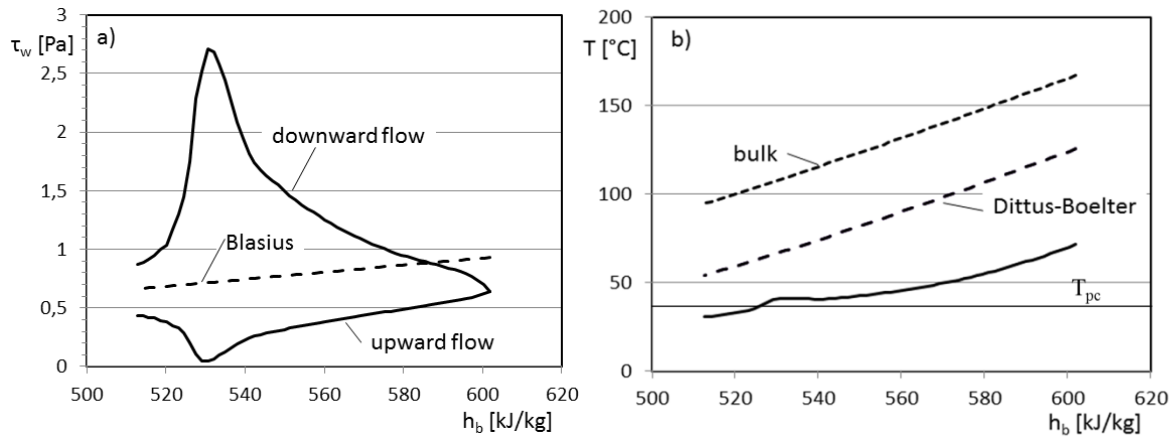
Figure 5: a) Wall shear stress and b) wall temperature with a cooled wall at p = 8 MPa, D = 2 mm, G = 166 kg/m^{2}s, q$_w$ = 30.8 kW/m^2, T$_{in}$ =165.8 °C. Comparison wth the Blasius and Dittus-Boelter Correlations based on bulk properties.
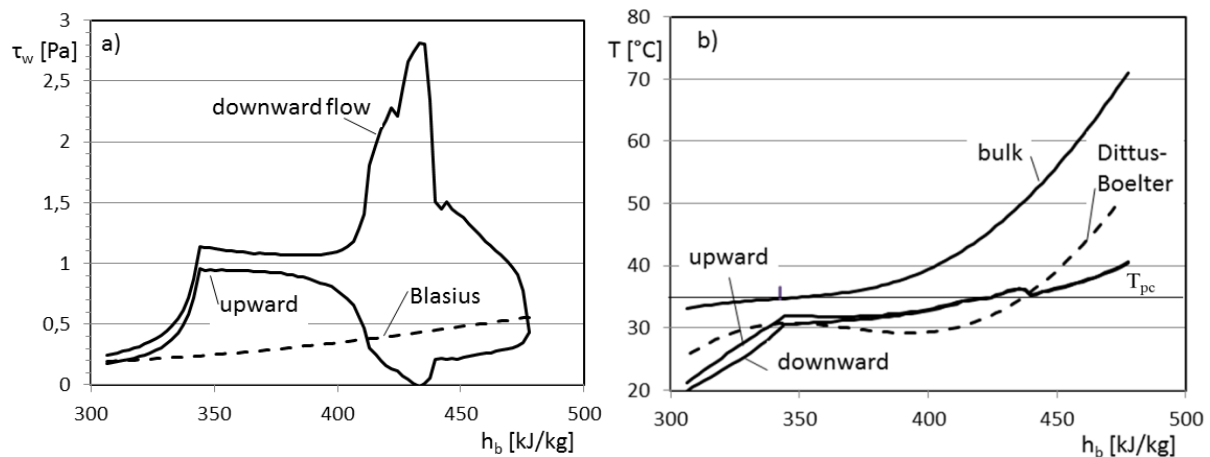

Figure 6: a) Wall shear stress and b) wall temperature with a cooled wall at p = 8 MPa, D = 2 mm, G = 166 kg/m^{2}s, q$_w$ = 15.4 kW/m^2, T$_{in}$ =69.8 °C. Comparison wth the Blasius and Dittus-Boelter Correlations based on bulk properties.

4. Conclusion

The extended two-layer model has the potential to predict the flow in compact heat exchangers for heated or cooled walls, both for upward and downward flow. Due to using only a small number of cases for the calibration of the model, additional validation work remains necessary to improve its reliability and accuracy.

In order to promote the understanding of the flow in the low-temperature recuperator and the reject-heat exchanger of the sCO$_2$ power cycle [1], we have made sample calculations with constant wall heat flux. At a pressure of 80 bars the predictions of the wall temperature and the wall shear stress deviate significantly from constant-property correlations.

The decision whether the flow in a heat exchanger should designed to be upward or downward can be supported by our data. Horizontal flow is not within the capability of our theory, however see [15]. For the high-pressure side, downward flow is favourable because of the lower wall shear stress compared to upward flow. For the low pressure side downward flow may lead to very small (almost zero) wall shear stress at 80 bars. Systematic computations of downward flow at 77 bars could not be performed due to negative wall shear stress in the case of downward flow with cooling. This does not occur in the case of upward flow.

5. References

[1] V. Dostal, M.J. Driscoll, and P. Hejzlar: A supercritical carbon dioxide cycle for next generation nuclear reactors, MIT-ANP-TR-100, (2004)

[2] J.D. Jackson, and W.B. Hall: Forced convection heat transfer to fluids at super-critical pressure. Turbulent forced convection in channels and bundles, Hemisphere, 563-611, (1979)

[3] H. Kim, Y.Y. Bae, H.E. Kim, J.H. Soong, and B.H. Cho: Experimental Investigation on the Heat transfer characteristics on a vertical upward flow of supercritical CO_2, Proc. ICAPP '06, Reno, NV, June 4-8, 2006

[4] J. Y. Yoo: The turbulent flows of supercritical fluids with heat transfer, Ann. Rev. Fluid Mech., 495–525, (2013)

[5] I.L. Pioro, H.F. Khartabil and R.B. Duffey: Heat transfer to supercritical fluids flowing in channels - empirical correlations (Survey), Nucl. Eng. and Design 230, 69-91, (2006)

[6] D. M. McEligot, and J. D. Jackson: 'Deterioration' criteria for convective heat transfer in gas flow through non-circular ducts, Nucl. Eng. and Design 232, 327–333, (2004)

[7] J. H. Bae, J.Y. Yoo, and H. Choi, Direct numerical simulation of turbulent supercritical flows with heat transfer, Physics of Fluids 17, 105104, (2005)

[8] Xu Chu, and E. Laurien: Direct numerical simulation of heated turbulent pipe flow at supercritical pressure, Journal of Nuclear Engineering and Radiation Science, to appear 2016

[9] L. Prandtl, Eine Beziehung zwischen Wärmeaustausch und Strömungswiderstand der Flüssigkeit, Physik. Z. 11, 1072-1078, (1910)

[10] W. Kays, M. Crawford, and B. Weigand: Convective heat and mass transfer, McGraw-Hill, New York, International Edition 2005

[11] B.A. Kader: Temperature and concentration profiles in fully turbulent boundary layers, Int. J. Heat and Mass Transfer 24, 1541-1544 (1981)

[12] E. Laurien: Implicit model equation for hydraulic resistance and heat transfer including wall roughness, Journal of Nuclear Engineering and Radiation Science, to appear 2016

[13] E. W. Lemmon, M. L. Huber, and M. O. McLinden: Thermophysical Properties Division, National Institute of Standards and Technology, Boulder, CO 80305 (2010)

[14] D.M. McEligot, and E. Laurien, Insight from simple heat transfer models, The 7th International Symposium on Supercritical Water-Cooled Reactors (ISSCWR-7), Helsinki, Finland, 15-18 March, 2015

[15] S. Pandey, and E. Laurien, Heat transfer analysis at supercritical pressure using two layer theory, The Journal of Supercritical Fluids, Volume 109, Pages 80-86, ISSN 0896-8446, March 2016.

[16] X. Chu, and E. Laurien: Inflow Effect to Heat Transfer of Pipe Flow with CO_2 at supercritical Pressure, this conference.

[17] P.X. Jiang, Y Zhang, C.R. Zhao, R.F. Shi, Convection heat transfer of CO_2 at supercritical pressures in a vertical mini tube at relatively low reynolds numbers, Experimental Thermal and Fluid Science 32, 1628–1637, (2008)

NOMENCLATURE

Non-dimensional parameters

Gr	-	Grashof number, $\rho^2 D^3 g\beta \,|T_b-T_w|/\mu^2$
K_v	-	acceleration parameter

$$K_v = \frac{4q_w\mu_b u_m}{GD\rho_b^2}\left.\frac{\partial\rho}{\partial h}\right|_b \quad ; \quad \left.\frac{\partial\rho}{\partial h}\right|_b = \frac{\rho_b\beta_b}{c_{pb}}$$

Nu	-	Nusselt number, $q_w D/|T_w-T_b|/k$
Pr	-	Prandtl number, $\mu\, c_p/k$
Re	-	Reynolds number, $\rho\, u_m D/\mu$
Ri	-	Richardson number, Ri = Gr/Re^2

Latin symbols

c_p	kJ/kg K	specific heat capacity at constant pressure
D	m	pipe diameter, D = 2R
g	m/s^2	gravity acceleration
G	kg/m^{2}s	mass flux per unit area
h	kJ/kg	specific enthalpy
k	W/m K	thermal conductivity
p	MPa	pressure
q	W/m^2	heat flux per unit area
r	m	radial coordinate
R	m	pipe radius
T	°C, K	temperature
u	m/s	streamwise velocity
y	m	distance from the pipe wall

Greek symbols

β	1/K	thermal expansion coefficient
κ	-	von-Karman constant, 0.41
λ	-	darcy pipe friction coefficient
ρ	kg/m^3	density
τ	Pa	shear stress

μ	$Pa\,s$	dynamic viscosity

Indices

|		
b		bulk
$+b$		wall unit based on bulk properties
cl		centreline
cs		laminar, conducting sub-layer
in		pipe inlet
m		mean, cross-sectional average
mod		modified to take account of buoyancy
pc		pseudo-critical, where c_p has its maximum
t		turbulence
$turb$		turbulent wall layer
vs		laminar, viscous sub-layer
w		wall
$+w$		wall unit based on wall properties
τ		wall friction

SHORT BIOGRAPHY INTRODUCTION OF AUTHOR(S)

Dr. Eckart Laurien is full time professor at Institute of Nuclear Technology and Energy System (IKE), University of Stuttgart, Germany.

Mr. Sandeep Pandey is currently working as a doctoral research scholar at IKE, University of Stuttgart, Germany. He holds Master of Technology in Energy Studies from Indian Institute of Technology Delhi, India.
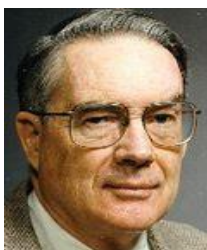
Dr. D.M. McEligot is Distinguished Visiting Professor, Nuclear Engineering, University of Idaho.